VAN BENNEKOM, A., MATTHEWS, L. M., TARBOTON, J. N., and ROBINSON, F. P. A. The effect of martensite content on the corrosion and mechanical properties of dual-phase 12 per cent Cr steels. *INFACON 6. Proceedings of the 1st International Chromium Steel and Alloys Congress, Cape Town.* Volume 2. Johannesburg, SAIMM, 1992. pp. 157–163.

The Effect of Martensite Content on the Corrosion and Mechanical Properties of Dual-phase 12 per cent Cr Steels

A. VAN BENNEKOM*, L. M. MATTHEWS†, J. N. TARBOTON†, and F. P. A. ROBINSON*

**University of the Witwatersrand, Johannesburg, South Africa*
†Middelburg Steel & Alloys, Middelburg, South Africa

Low-carbon dual-phase steels are well known for their improved strength and toughness due to the presence of ferrite and martensite. This paper investigates the extent to which this phenomenon occurs in dual-phase 12 per cent Cr alloys after they have been held above the A_1 temperature and then quenched.

It was found that the mechanical properties can be described reasonably well by a simple linear regression between the property of interest and the volume fraction of martensite. This does not apply to the impact strength, which is very sensitive to microstructural features. The resistance to general corrosion is decreased by the presence of martensite, but the pitting potential also decreases for an increase in martensite content. Likewise, the stabilization of this type of alloy by the addition of either titanium or niobium brings about a reduction in pitting potential.

Introduction

The use of dual-phase (ferrite and martensite) low-carbon steel has been extensive since 1975[1]. Hayami and Furukawa[2] were the first to publish a description of its chemistry, microstructure, and mechanical properties. They showed that the combination of ferrite and martensite in these steels increased both their ductility and their strength, as indicated by the higher elongation values at higher tensile strength. Because of the wide range of applications and the large tonnage of low-carbon mild steels used in industry, much research has been conducted on the effect of the martensite content and morphology on the mechanical properties of low-carbon dual-phase steels[1,3-5]. These studies revealed that, for optimum strength and toughness, a fine ferrite grain size and a dispersion of small islands of martensite are required, usually amounting to a martensite content of about 20 to 30 per cent for low-carbon dual-phase steels. Certain of these studies included work on different processing routes to yield the same amount of martensite. A particularly suitable method of obtaining such a structure in sheet material is by on-line annealing at temperatures slightly above the A_{C1} temperature, followed by rapid cooling depending on the transformation (or hardenability) characteristics of the material.

The mixing of constituents in materials to give the beneficial effects of various phases, such as composites reinforced with fibre particles and low-carbon dual-phase steels, has also been used in the development of stainless steels. The best-known of these are the range of micro-duplex ferrite–austenite steels (22 to 27 per cent Cr, 3 to 5 per cent Ni, and 3 to 4 per cent Mo), which have received much attention[6]. The combination of phases in these alloys results in superior resistance to stress–corrosion (due to the presence of ferrite), and better toughness (due to the presence of austenite).

A less well-known development is that of 12 per cent Cr steels made under the registered trade names of 3CR12[7], DIN 1.4003, and ACX585 (Acerinox). To date, the main use of the concept of two phases in these alloys has been the formation of a ferrite–austenite structure at high temperature to ensure toughness in the heat-affected zone (HAZ) after welding. The austenite present at the high temperatures near the fusion line prevents the excessive grain growth commonly found in fully ferritic steels[8]. Another possible advantage offered by this steel is its improved wet-abrasion properties[9]. The 12 per cent Cr level limits corrosion under wet conditions, and the abrasion resistance arises from the presence of the transformation product, which is usually a mixture of martensite and ferrite together with hard carbides, depending on the cooling rate. In many cases, the martensite is tempered by annealing at temperatures below the A_{C1}, resulting in the formation of a ferrite and carbide structure. More recently, this work was extended to alloys containing higher amounts of chromium in which a mixture of ferrite and martensite would still afford the beneficial properties described above, but with much improved resistance to corrosion[10].

The present paper describes the effect, on the mechanical and corrosion properties of specimens from three production heats with different chemical compositions, after annealing at temperatures above the A_1 followed by rapid cooling. The properties are influenced by the percentage martensite formed at the various temperatures, and it will be seen that a range of desired properties can be obtained by the selection of suitable times at temperatures above the A_1 temperature.

TABLE I
CHEMICAL COMPOSITION AND TRANSFORMATION TEMPERATURES FOR THE SPECIMEN ALLOYS

ID	C %	S %	P %	Mn %	Si %	Ti %	Cr %	Ni %	Nb %	N p.p.m.	A_{C1} °C	M_s °C	Stab. ratio*
TI	0,018	0,004	0,030	1,11	0,80	0,365	11,83	0,56	0,003	191	822	488	9,9
US	0,023	0,006	0,027	0,98	0,40	0,005	11,55	0,19	0,004	138	797	398	0,24
NB	0,021	0,005	0,030	0,94	0,87	0,004	12,18	0,17	0,286	325	821	395	5,4

* The stabilization ratio is (Ti+Nb)/(C+N)

Experimental

Heat Treatment

The test samples used for this research were taken from plate material that originated from production melts. The identification, compositions, A_{C1} and M_s temperatures, and stabilization ratios—(Ti+Nb)/(C+N)—are given in Table I. The table shows that the essential differences between these alloys is the presence or absence of stabilization. There are also some minor changes in the other elements, and the effects of these are discussed in more detail by Hewitt[11].

Since the hot-rolling schedules were different for these alloys, all the plates were first annealed at 780 °C for 30 minutes to produce a ferrite-plus-carbide structure. Following the annealing treatment, the steels were held for 20 minutes at the following temperatures: 780, 810, 815, 820, 825, 830, 840, 850, 900, 950, and 1000 °C. After air-cooling from these temperatures, the specimens were prepared for the various tests.

Mechanical Testing

Mechanical testing was performed only on the niobium-stabilized and unstabilized alloys (marked NB and US respectively). Tensile tests were conducted according to ASTM A370 using sheet-type tensile specimens that were 12,5 mm wide of 50 mm gauge length. The specimens were machined transverse to the rolling direction, and two tests were conducted on each heat-treated sample.

As a test of impact toughness, Charpy V-notch tests were run according to ASTM E23. The US steels were of sample size 10 x 10 x 55 mm, while specimens measuring 6 x 10 x 55 mm were used for the NB alloys. All the specimens had been machined transverse to the rolling direction, with the notches parallel to the rolling direction to produce crack-propagation parallel to the rolling direction. At least three tests were conducted for each heat-treated condition. All the tests were conducted at room temperature.

Corrosion Testing

Specimens of the experimental stainless steels were prepared as follows for electrochemical corrosion testing: the plate material was sectioned, an insulated wire was soldered onto the back of the specimen for electrical contact, and the specimen was then coated with fibreglass resin. The surfaces of the specimens were then progressively wet-ground and finally polished to a 1 μm diamond finish. The edges of the exposed surface were then coated with Prakley™ quick-setting glue to prevent crevice-corrosion effects from interfering with the test results.

The exposed area was measured accurately and the desired corrosion scan carried out. On completion of the scans, the results were evaluated statistically, and outlying results were rejected on the basis of a Q-test and 95 per cent confidence level. When results were rejected, additional tests were performed so that an average of three valid data points could be used for the plotting of the graphs. All the potentials referred to in this paper are quoted relative to the saturated calomel reference electrode (SCE).

Potentiodynamic Testing

Potentiodynamic polarization scans were performed in triplicate according to ASTM Standard G5, additional tests being performed if necessary. The tests were conducted in a de-aerated 0,1N H_2SO_4 solution at 25 °C, using a Princeton 273 corrosion-measurement system. These experiments were used to obtain general corrosion rates for the specimens by the linear-polarization and Tafel-slope technique. The scans obtained from these tests also give an indication of the overall corrosion behaviour of the specimens at various potentials, i.e. active and passive ranges can be identified, as well as the regions of pitting and general corrosion.

Pitting-corrosion Scans

De-aerated 0,025 N NaCl and 0,025 N Na_2SO_4 solution at 25 °C was found to give well-defined pitting potentials for this type of alloy. This solution also gave rise to pitting potentials below 1200 mV, which was required because it was felt that pitting values higher than this could have been mistaken for the breakdown of passive films. Before the tests, the specimens were allowed to remain in the test solution in the corrosion flask for 1 hour to stabilize and reach their free corrosion potential. The scans were initiated at E_{Corr}, and were reversed above the pitting potential at a current density of 500 μA/cm^2 using a scan rate of 1 mV/s. The specimens were examined under a stereo-microscope on completion of the tests to verify the absence of crevice attack and to ensure that pitting had occurred. Triplicate scans were carried out on each of the specimens, additional tests being performed if necessary.

Scanning Electron Microscopy

Selected samples from both the general- and the pitting-corrosion tests were examined under the scanning electron microscope (SEM).

Results

Microstructure

Figure 1 shows the percentage martensite formed for the different alloys after they had been held at the given temperatures for 20 minutes. The phase percentages of martensite and ferrite quoted were determined by means of image analysis following etching in a 10 N KOH solution at room temperature. The unstabilized material, which has a lower A_{C1} temperature, is seen to form martensite very rapidly for a small increase above the A_{C1} temperature. The volume

fraction of martensite formed by heat treatment is seen to peak at 950 °C for the niobium-stabilized and unstabilized steel. The titanium-stabilized steel appears to reach a maximum at 1000 °C or higher temperatures. Other titanium-stabilized steels of similar composition were found to have maximum austenite in the range 1000 to 1050 °C. The maximum percentage martensite formed for the unstabilized steel is 92 per cent and, for the niobium-stabilized steel, it is 33 per cent. The martensite content for the titanium-stabilized steel, after water quenching from 1000 °C, is 25 per cent. The lower amount of martensite formed in the stabilized materials is due to the formation of Ti(C,N) or Nb(C,N), which effectively reduces carbon and nitrogen, both elements being very powerful austenite stabilizers. The removal of these two elements reduces the amount of austenite formed at high temperatures.

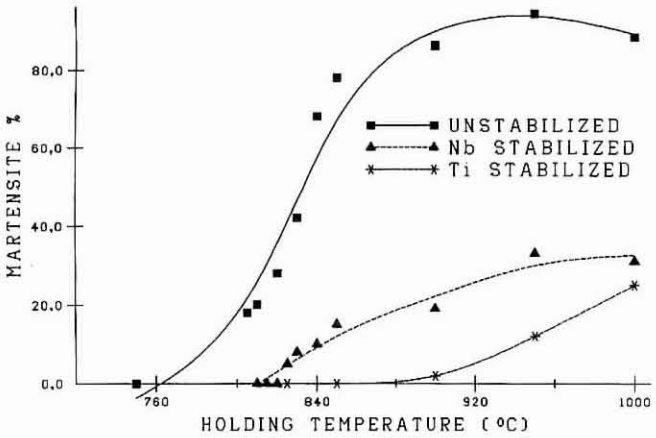

FIGURE 1. Martensite formation as a function of holding at different temperatures

The distribution of martensite (approximately 30 per cent) in the niobium-stabilized material is shown in Figure 2. The actual distribution was found to be strongly influenced by the microstructure prior to austenitization. A hot-rolled structure prior to austenitization very often leads to an elongated martensite morphology — in this case, even after the annealing process at 750 °C. This indicates that Nb(C,N) has precipitated out and is effectively pinning the grain boundaries. Figure 3 shows the martensite distribution for the unstabilized material at a martensite content of approximately 95 per cent.

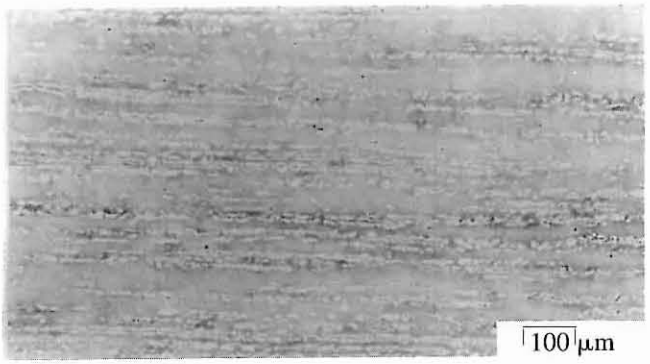

FIGURE 2. Typical martensite distribution in the niobium-stabilized material. Ferrite occurs in clearly delineated islands (white). (Etched in 10 N KOH)

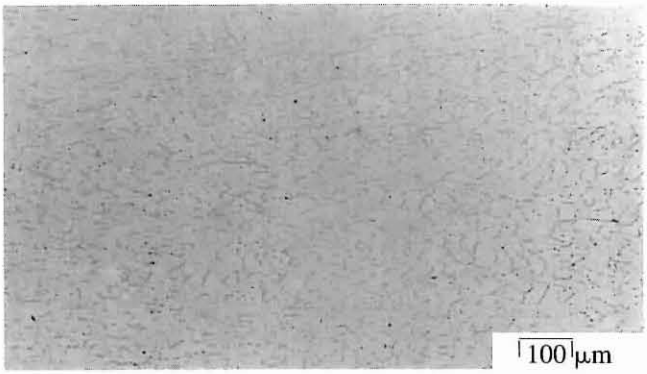

FIGURE 3. Micrograph showing the typical distribution of martensite and ferrite in the unstabilized alloy (Etched in 10 N KOH)

Results of the Mechanical Tests

The results of tensile tests for both the unstabilized and the stabilized material are shown in Figure 4. From this diagram it is evident that an increase in the martensite content leads to an increase in both the 0,2 per cent proof stress and the tensile strength. The relationship is near-linear, and the same line fits both the compositions used. Regression analysis gives the following relationship between the martensite content and the proof stress and tensile strength (*UTS*):

UTS (MPa) = 460 + 549 * (V_m) and

0,2% proof stress (MPa) = 294 + 585 * (V_m),

where V_m is the volume fraction of martensite. Correlation coefficients of 0,97 were obtained in both cases.

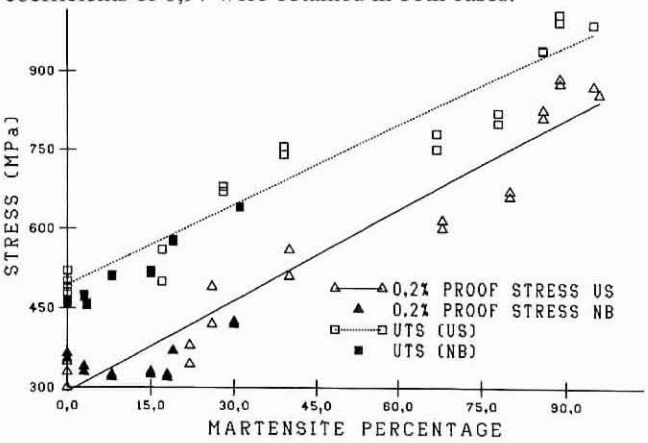

FIGURE 4. 0,2 per cent proof stress and tensile strength as a function of martensite content. The linear-regression curves are drawn in. The data points for NB and US material are included

These relationships indicate that, in the presence of martensite, stabilization has very little effect on the proof stress and tensile strength of the material. This is expected for alloys that have been annealed at 750 °C. The annealing process would result in the precipitation of Nb(C,N), which would remain in the matrix even after subsequent heat treatments in the dual-phase austenite and ferrite region. This is largely because these temperatures are below the dissolution temperatures for titanium and niobium carbo-nitrides.

Figure 5 shows the effect of an increase in the martensite content on elongation and hardness. As for the tensile properties, equations can be derived from regression analysis to predict the drop in elongation and increase in hardness associated with an increase in martensite content. As was found for the strength properties, the effect of stabilization appears to have very little influence on the elongation and

hardness of these alloys in the presence of martensite. The results of the linear-regression analysis are as follows:

Elongation (%) = 31,2 – 16,5 * V_m

Hardness (HBN) = 162 + 170 * V_m,

where V_m is the volume fraction of martensite, and elongation is the percentage in a specimen of 50 mm gauge length. The correlation coefficients are 0,86 and 0,96 respectively.

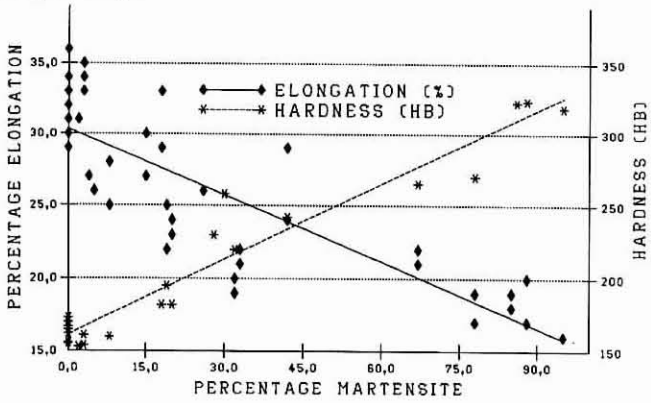

FIGURE 5. Elongation and Brinell hardness as a function of the martensite present. The data points for both the US and the NB alloys are given

The results obtained are similar to those typically found for low-carbon dual-phase steels. Figure 6 compares the results of this study with those published for low-carbon steels[1,3,5]. The banded regions show the scatter of proof and tensile strengths as a function of martensite content in the low-carbon dual-phase steel. The essential difference is that low-carbon dual-phase steels have a lower proof stress for a fully ferritic structure, and show a more rapid increase in tensile strength for an increase in martensite content. This higher proof stress in the 12 per cent Cr steel is the result of substitutional solid-solution hardening by the chromium.

The more rapid increase in tensile strength and proof stress due to an increase in martensite content is due to the overall higher carbon contents (typically 0,1 per cent) of the low-carbon dual-phase steels in comparison with the 12 per cent

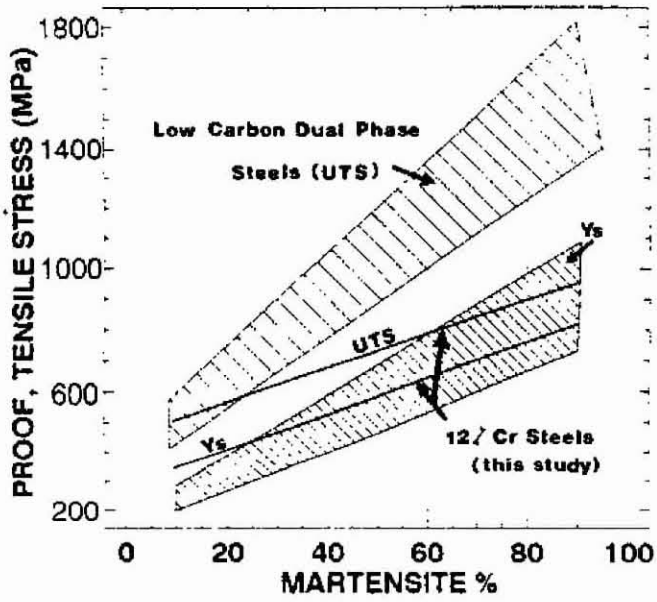

FIGURE 6. Comparison of the influence of the martensite content of 12 per cent Cr steels with that of low-carbon dual-phase steels[1,3,5]

Cr steels. The martensite in the low-carbon dual-phase steel is harder, and has a higher strength than that in the 12 per cent Cr steel, as indicated by the difference in strength for fully martensitic material, viz low-carbon dual-phase steel 1400 to 1800 MPa, and 12 per cent Cr steel approximately 1000 MPa.

The results of the impact tests, Figure 7, show a distinct difference between the stabilized and the unstabilized steels, the unstabilized steels having a much higher impact value for an equivalent martensite content. The difference in microstructure as observed in Figures 2 and 3 is the factor contributing to the difference in impact behaviour. The laminated martensite distribution in the stabilized steel leads to the poorer impact properties. At the lower percentages of martensite, the Nb(C,N) precipitation and some grain refinement increase the toughness.

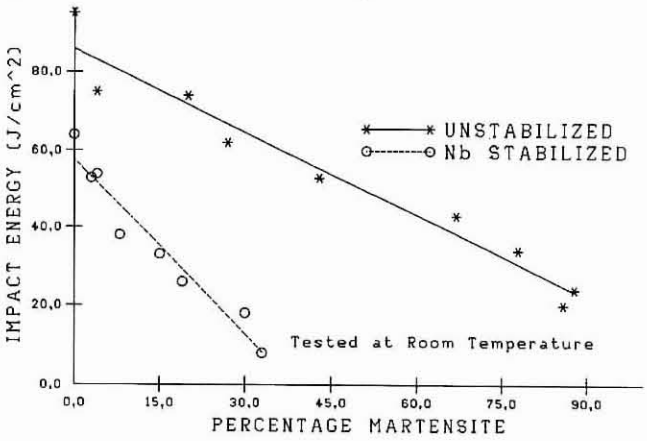

FIGURE 7. Impact energies for the unstabilized and niobium-stabilized alloys. The stabilized alloy has a lower impact energy

Results of Corrosion Tests

All three alloys were evaluated for corrosion resistance as a function of martensite content. The results of the pitting tests showed that the pitting potentials of the unstabilized alloy are much lower than those of the stabilized alloys, indicating that stabilization of the alloy by either niobium or titanium is beneficial. The titanium-stabilized alloy has a higher stabilization ratio (Table I) than the niobium-stabilized alloy, and this is highlighted by the higher pitting potentials measured in the pitting tests. However, titanium stabilization is not always beneficial since it can affect the mechanical properties adversely. The large cuboidal titanium carbo-nitride precipitates formed lead to the formation of voids during deformation, and can also give rise to poor surface quality in rolled products, as indicated by the formation of skin laminations.

Overlays of the general- and pitting-corrosion scans are shown in Figures 8 and 9. The overlay of the pitting scans in Figure 8 and the data presented in Table II clearly show that the pitting potentials (E_p) increase with increasing martensite content. All the pitting scans contain a substantial hysteresis loop between the forward and the reverse scans, indicating that these alloys would be susceptible to crevice corrosion in this environment. The overlay of representative general-corrosion scans in Figure 9 indicates that the free corrosion potentials (E_{Corr}) decrease slightly as the martensite content increases, while the densities of the critical current (I_C) and the passive current (I_p) increase slightly. The general-corrosion rates of the alloys presented in Table III give an indication of the spread of the data obtained

TABLE II
PITTING POTENTIALS OF THE ALLOYS TESTED IN
0,25 N NaCl + 0,25 N Na_2SO_4

Sample	Martensite %	Pitting potentials, mV vs SCE			
		Test 1	Test 2	Test 3	Average
Unstabilized alloy	0	461	478	472	470
	23,5	501	506	489	498
	40	552	535	537	541
	65	567	555	549	557
	83,5	578	586	572	579
	85	589	579	572	580
Niobium-stabilized alloy	0	525	540	534	533
	0	560	550	543	551
	9,5	572	553	567	564
	15,6	572	561	577	570
	23,7	615	607	617	613
Titanium-stabilized alloy	0	660	668	674	667
	0	684	691	676	684
	0	694	688	702	695
	1,7	708	718	717	714
	10,3	755	738	745	746

TABLE III
GENERAL-CORROSION RATES OF THE ALLOYS TESTED IN
0,1 N H_2SO_4

Sample	Martensite %	Corrosion rates, mpy			
		Test 1	Test 2	Test 3	Average
Unstabilized alloy	0	172	183	179	178
	23,5	191	201	207	200
	40	226	240	223	230
	65	250	240	235	242
	83,5	257	262	264	260
	85	256	265	266	262
Niobium-stabilized alloy	0	197	210	211	206
	0	221	222	218	220
	9,5	252	241	254	249
	15,6	252	261	247	253
	23,7	289	304	295	296
Titanium-stabilized alloy	0	164	183	180	176
	0	177	192	184	185
	0	185	194	199	193
	1,7	192	204	212	203
	10,3	218	232	220	223

from the corrosion results. These factors indicate that the general-corrosion resistance of the alloys decreases as the martensite content increases.

When the general-corrosion rates in Figures 10 to 12 are compared, it can be seen that the lowest corrosion rates were measured on the fully annealed samples containing no martensite. The reason for this is that ferrite, the only phase present in fully annealed 12 per cent Cr steels, is more corrosion-resistant than martensite[12]. The corrosion rate would therefore be expected to increase, as indeed it does, as the martensite content increases.

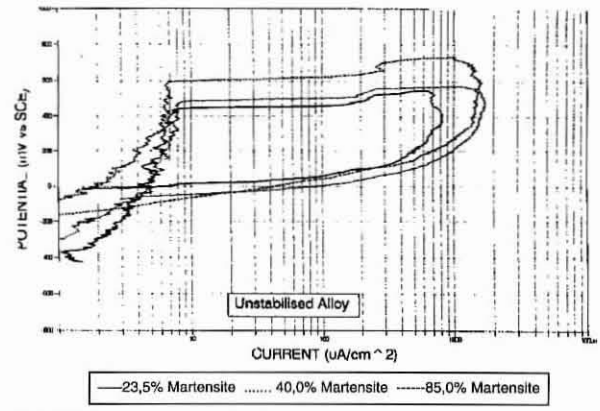

FIGURE 8. An overlay of pitting scans obtained from the unstabilized alloy

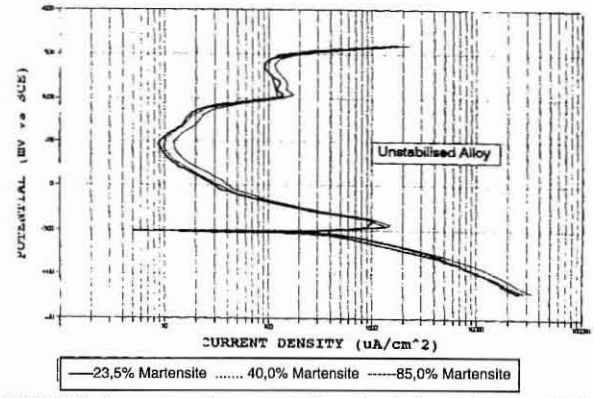

FIGURE 9. An overlay of representative potentiodynamic scans obtained from the unstabilized alloy

The pitting potentials for these alloys that are plotted on the same graphs show the opposite trend in that they decrease as the martensite content increases. Higher pitting potentials indicate greater resistance to pitting corrosion. This implies that the presence of increasing quantities of martensite increases the resistance of these alloys to pitting corrosion.

When the potentiodynamic samples were examined under the electron microscope, no preferential general corrosion of the martensite was observed; instead, both phases were seen to have corroded fairly severely. On examination of these specimens under the electron microscope, it was found that most of the pitting had occurred in regions of high grain-

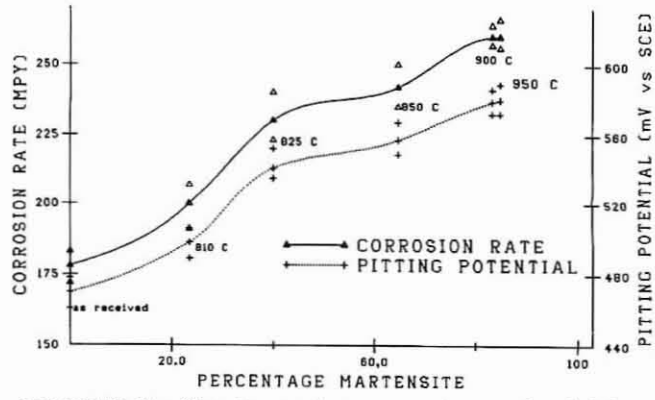

FIGURE 10. The effect of martensite content on the general- and pitting-corrosion properties of the unstabilized alloy. The temperatures indicate the holding temperatures after annealing

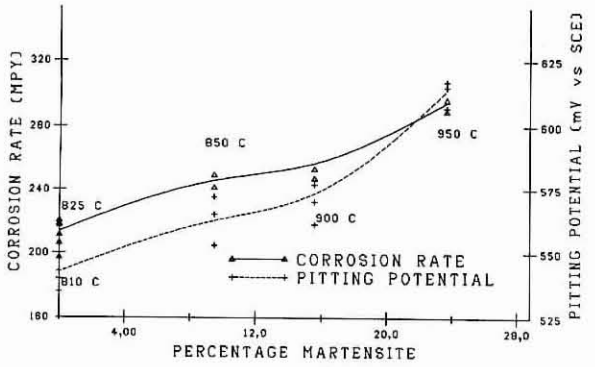

FIGURE 11. The effect of the martensite content on the general- and pitting-corrosion properties of the niobium-stabilized alloy. The temperatures indicate the holding temperatures after annealing

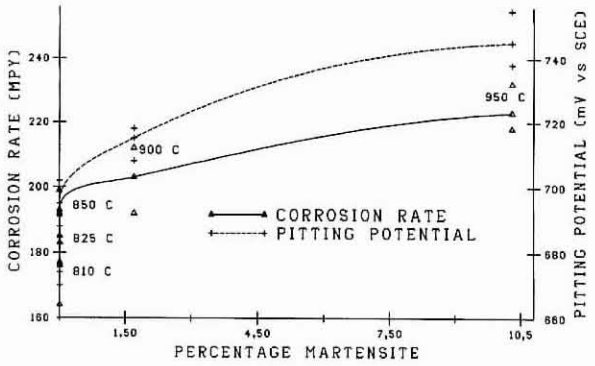

FIGURE 12. The effect of martensite content on the general- and pitting-corrosion properties of the titanium-stabilized alloy. The temperatures indicate the holding temperatures after annealing

boundary density, triple points, and manganese sulphide inclusions. Some of the pits were seen to contain irregularly shaped precipitates, as shown in Figure 13. EDS analyses of these precipitates showed them to be rich in chromium (Figure 14), indicating that they were probably chromium carbides of the type $M_{23}C_6$, as had been found in a previous investigation[12]. The sulphur and chloride peaks detected on the analyses of the precipitates probably originated from the pitting-test solution, but could also have been associated with the precipitate (especially the sulphur).

This could be a possible reason why the unstabilized alloy had the lowest pitting potentials. The pitting potentials were found to increase, while the number of pits observed

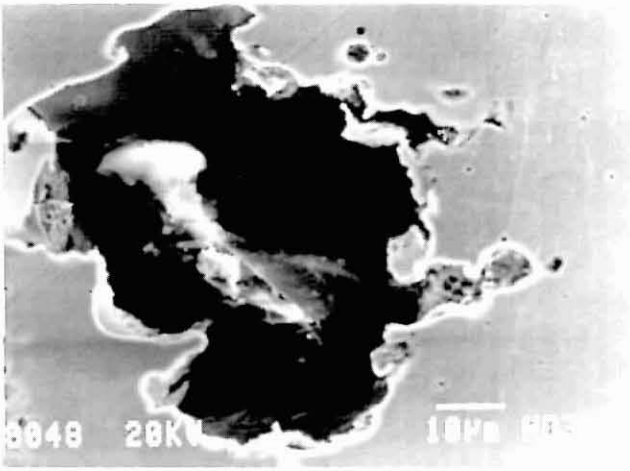

FIGURE 13. Electron micrograph of the chromium-rich precipitates observed inside the corrosion pits

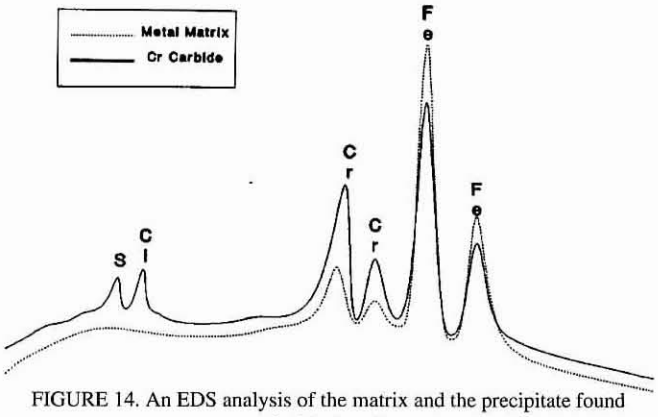

FIGURE 14. An EDS analysis of the matrix and the precipitate found inside the pit

after the pitting tests were found to decrease as the martensite content increased. This can be explained by the fact that, when 12 per cent Cr alloys are heated above the A_1 temperature, the carbides dissolve. Carbon has a much greater solubility in austenite and therefore dissolves in the austenite. It is retained in the austenite, which, on cooling, transforms to martensite. This results in less free carbon being available for the formation of discontinuous chromium carbides, which have been shown to accelerate pitting corrosion[12]. It should be noted that the chromium carbides in question are relatively small and discontinuous, and would not render the alloy susceptible to intergranular attack, i.e. the alloy is not sensitized.

Discussion

From the results obtained, it is obvious that, once a suitable composition has been decided on, for example in terms of the maximum austenite content obtainable at high temperatures, the alloy can be heat-treated to give pre-selected mechanical and corrosion properties. From the points of view of both mechanical and corrosion properties, there are two factors that have to be weighed against each other.

The martensite content of these steels can be raised to increase the strength, but this has to be kept below a certain limit to ensure suitable toughness in terms of both elongation and impact strength. The graphs and the simple linear regressions show that, for a minimum elongation of 20 per cent (if this is the chosen criterion), it is advisable to keep the martensite content below 40 per cent. This would give a proof stress of approximately 530 MPa, a tensile strength of 680 MPa, and impact energy in excess of 50 J/cm^2.

From a corrosion point of view, the two criteria are pitting- and general-corrosion resistance. The general-corrosion resistance was found to deteriorate with an increase in martensite but is relatively unaffected by stabilization, while the pitting resistance is strongly influenced by stabilization. Industrial environments do not result only in pitting corrosion or general corrosion in a stainless steel, but usually result in a combination of general and pitting corrosion. This implies that a compromise must be found between resistance to pitting and resistance to general corrosion. In the unstabilized 12 per cent Cr alloy, this compromise appears to be obtained with an alloy containing between 40 and 60 per cent martensite, as shown in Figure 10. Stabilization would bring about a relative improvement in the pitting resistance, but would not greatly affect the

martensite content required to give the best compromise for corrosion resistance.

Conclusions

- As a first estimate, the proof stress, tensile stress, hardness, and elongation can be described by a linear approximation of the percentage martensite present after quenching from above the A_1 temperature.
- The mechanical properties are unaffected by stabilization on quenching from above the A_1 temperature.
- The impact strength is strongly affected by stabilization. This can be ascribed to the effect of stabilization on the distribution of martensite in the stabilized material.
- Corrosion pits are found to initiate preferentially around chromium-rich carbides.
- Stabilization is beneficial from a pitting-corrosion point of view in that it reduces the amount of chromium carbide precipitation, which in turn reduces the number of pit-initiation sites.
- An increase in the martensite content decreases the resistance to general corrosion, while the resistance to pitting corrosion is increased.
- The best compromise between resistance to general corrosion and that to pitting corrosion is obtained at a martensite level of between 40 and 60 per cent.
- Stabilization of these alloys is beneficial from a corrosion point of view, and a combination of titanium and niobium stabilization could be considered in order to bring about an improvement in the mechanical properties of the stabilized alloys.

References

1. Owen, W.S. (1975). Can a simple heat treatment help to save Detroit? *Metals Technology*, vol. 7, no. 1, pp. 1–13.
2. Hayami, S., and Furukawa, T. (1977). *Microalloying 75*, New York, Union Carbide Corp., vol. 1, 78 pp.
3. Marder, A. R. (1982). Deformation characteristics of dual-phase steels. *Met. Trans. A*, vol. 13A, pp. 85–92.
4. Davies, R. G. (1978). The deformation behaviour of a vanadium-strengthened dual phase steel. *Met. Trans. A*, vol. 9A, pp. 41–52.
5. Balliger, N. K., and Gladman, T. (1981). Work hardening of dual-phase steels. *Metal Science*, Mar., pp. 95–108.
6. Solomon, H. D., and Devine, T. M. (1983). Duplex stainless steels — a tale of two phases. *Duplex Stainless Steels*, Lula (ed.), New York, ASM, pp. 693–756.
7. Middelburg Steel & Alloys (Pty) Ltd. (1978). A corrosion resistant ferritic steel composition. *S. Afr. Pat.* 78/4764, 11 pp.
8. Hoffman, J. P. (1984). The welding metallurgy of a titanium stabilized 12 per cent chromium ferritic–martensitic steel. *International Conference on New Developments in Stainless Steel Technology*, ASM, Metals Park (Ohio), pp. 1–13.
9. Barker, K. C., and Ball, A. (1989). Synergistic abrasive–corrosive wear of chromium containing steels. *Br. Corros. J.*, vol. 24, no. 3, pp. 222–228.
10. Miyakusu, K., Fujimoto, H., and Uematsu, Y. (1991). Effect of alloying elements and heat treatment on microstructures and mechanical properties of ferrite–martensite dual phase stainless steel sheets. *Stainless Steel 91, Chiba, Japan*, ISIJ, Tokyo, pp. 565–572.
11. Hewitt, J. (1992). High–Chromium Controlled–Hardenability Steels. Paper Presented at this congress INFACON 6, 1992.
12. Van Bennekom, A. (1990). The corrosion and mechanical properties of modified 3CR12 type alloys. M.Sc. thesis, University of the Witwatersrand, Johannesburg.